Digest Journal of Nanomaterials and Biostructures Vol. 9, No. 3, July – September 2014, p. 1021 - 1037

SURFACE MELTING AND THERMAL ABLATION PATTERNS INDUCED IN ENAMEL AND CEMENTUM BY10.6-μm TEA-CO_2LASER RADIATION. II. THEORETICAL MODELS FOR RADIATION-ENAMEL INTERACTIONS

E. A. PREOTEASA[a], I. MIHAILESCU[b*], E. S. PREOTEASA[c]
[a]*Horia Hulubei National Institute of Physics and Nuclear Engineering, Department of Life and Environment Physics, P.O. Box MG-6, 077125 Bucharest-Magurele, Romania*
[b]*National Institute for the Physics of Lasers, Plasma and Radiation, P.O. Box MG- , 077125 Bucharest-Magurele, Romania*
[c]*Helident Ltd. Dental Surgery, Bucharest, Romania*

To better understand the nature of the ultrastructural changes evidenced by SEM and AFM in the surface layer of dental enamel irradiated with the TEA-CO_2 laser at 75, 175 and 625 J/cm^2fluence – and foremost, the periodic patterns reported for the first time in Part I of this study – a theoretical analysis of the physical interactions has been carried out. The exponential or Langmuir-type saturation of the RMS roughness vs. fluence relationship points to the competition between the laser pulse melting of the surface layer and a 'relaxation' by own internal dynamics with an energy barrier which opposes to the external action. The energy balance of the interactions between the laser pulse and enamel suggests large lossesfrom the incident energy in the plasma formation. Models are suggested for the ultrastructural changesproduced by the non-polarized laser pulses with Gaussian profile at 625 J/cm^2 fluence.Theoretical predictions for resonant periodic structures based on the electrodynamical mechanism of diffraction and interference of laser radiation in the melted surface enamel layer fit excellently to the ~11 μm short length waves seen in the enamel with perpendicular prisms. The thermophysical description of the interaction between the laser pulse and the target evidences relationships between the resonant periodic structures, the pulse fluence threshold, the pulse duration and enamel's constants like specific vaporization heat and thermal diffusivity.The present results introduce our theoretical analysis as a powerful approach and encourage further developments.

(Received June 6, 2014; AcceptedAugust 13, 2014)

Keywords: TEA-CO_2 laser, Dental enamel, Prism orientation,Ablation pattern, Resonant periodic structures, Electrodynamic description, Thermophysical description.

1. Introduction

*General perspective*The experimental results from the first part of this study, henceforth refered to as Part I [1], evidenced a largevariety of ablation patterns produced by the TEA-CO_2 laser in the dental enamel at 75, 175 and 625 J/cm^2 nominal fluence; these are both new and similar to those already described in previous investigations. A number of theoretical models of the laser-induced effects are postulated in the present and following Part II and Part III.Among the patterns visualized by SEM, the concentric wave systems and their strongdependence of the enamel prisms' orientation as well as the resonant periodic structures (RPS,review in [2]) were the

* Corresponding author: ion.mihailescu@inflpr.ro

most remarkable ones. Both types of periodic patterns were not observed previously in dental enamel. The second ones were evidenced before in conducting metals, crystals and ceramic multilayered coatings, but in our study they were produced for the first time by laser irradiation of dental enamel as a particular biomineral tissue. Moreover, the AFM-measured roughness was showing an asymptotic saturation dependence on fluence, influenced by the orientation of enamel prisms. Similar effects were observed in the case of the ablation rate of hard dental tissues [3 – 6], bone [5, 7, 8], and non-biological materials [10], but this behaviour is not completely understood so far. In Parts II and III of our study, the general phenomenology of the laser-induced ultrastructural changes and their theoretical interpretation are discussed in detail.

The patterns of ~11 μm period produced only in enamel with perpendicular prisms by the unpolarized pulsed TEA-CO_2 laser radiation at 625 J/cm^2 fluence identified in Part I as RPS benefit here (Part II) by a privileged place for analysis based on theoretical models.However, in addition to this effect other aspects of the laser ablation are approached in Part II, for instance the asymptotic saturation of the roughness vs. fluence relationship. Concurrently, the concentric 'frozen waves' of ~42 and ~68 μm observed in the two types of enamel and recognized as non-resonant periodic structures (NRPS) will be discussed in Part III in the frame of new theoretical models.But there too, other phenomena will be treated in addition, like the plasma formation and its possible role in the calcination and characteristic ultrastructural configurations observed in enamel at the boundary of the laser spot, which were more complex than already described [9, 10].

*Experimental studies*Considerable endeavour has been made already aiming at a physical understanding of the complex interactions of the pulsed CO_2 and other lasers' radiation with the dental hard tissues([5, 11] and references therein). Among other, experimental studies include SEM, AFM and confocal microscopy of the ablation patterns [1, 3 – 9], measurements of ablation depth dependence on fluence in bone as a model for teeth [7, 8], examination of ablation pattern geometry and optical emission spectroscopy analysis of plasma from sound and carious enamel [4], FTIR[1] spectroscopy of collected particles ejected from enamel irradiated with a TEA-CO_2 laser [12], SEM-EDX evaluation of Ca/P ratio in laser-irradiated enamel [13], investigations of the crystallographic and chemical structure of the irradiated dental tissue by XRD [14, 15], IR spectrometry [16, 17] and Raman spectroscopy [18].

*Theoretical studies*Theoretical models and numerical calculations were elaborated to evaluate the temperature distribution and thermal effects caused by the CO_2 laser irradiation of teeth [19]. To understand the mechanisms involved in the pulsed laser ablation of enamel and dentine – opaque materials characterized by strong absorption and scattering – most models aim at computing primarily the light distribution and heat transport in the hard dental tissue. The main – but not unique – approach is based on the diffusion equation, which in general includes a heat source term in order to describe the evolution during the laser pulse, but takes a simpler form without this term for the evolution after the pulse. Basic mathematical aspects of this and other approximations – first-order scattering, Kubelka-Munk theory, Monte Carlo simulation of the random walk of photons in the tissue, inverse adding-doubling and finite element method were briefly described [20]. Other models which propose to treat the photon multiple scattering were a simple diffusion of a particular physical quantity provoked by its conjugated gradient [21] or the use of the classical molecular dynamics method for simulating the primary laser excitations and the vibrational relaxation of excited molecules of the tissue [22]. The mathematical difficulties in solving the partial derivatives diffusion equation are partly circumvented by using cylindrical coordinates accounting for the axial symmetry of the laser beam [23] or by using a one-dimensional diffusion equation, which is a good approximation since the laser spot diameter is much larger than the diffusion depth [24]. In the later study, by measurement of the hard tissue

[1]**Abbreviations and acronyms**

AFM – atomic force microscopy; FTIR spectrometry – Fourier transform infrared spectrometry; HA – hydroxyapatite; IR – infrared; NRPS –non-resonantperiodic structures; PIXE – particle-induced X-ray emission; RMS – root mean square; RPS– resonant periodic structures;SEM – scanning electron microscopy; SEM-EDX – SEM energy-dispersive X-ray spectrometry; TEA – transversally excited, atmospheric pressure; YAG– yttrium-aluminium-garnet ($Y_3Al_5O_{12}$); XRD – X-ray diffraction.

temperature decay following pulses of Er:YAG and Er,Cr:YSGG lasers and bybest fit of the 1D diffusion equation to all data, the ablative temperatures of enamel (600°C ± 50°C) and dentin (500°C ± 50°C) were determined. However, numerical solutions in teeth and other tissues are most frequently obtained by applying the Monte Carlo and finite volume methods to the diffusion equation (e.g. [23, 25, 26]). In the more general case the Pennes bio-heat transfer equation is used for the laser irradiation of various tissues. The numerical solutions of this equation in a non-dental tissue were obtained by the finite element method [27]. In another model the Pennes and the optical transport equation were solved in the diffusion approximation [28]. In a few models tissues were featured more realistically as anisotropic [29] and heterogeneous [30] media. Thus by use of finite-element models of the ablation produced by CO_2 (at 10.6 μm) and Er:YAG lasers (at 2.94 μm) accounting for the heterogeneous structure of enamel, the important role of pore and layer water at nm and μm scales for stress generation in enamel was evidenced, and effective operating parameters for dental laser ablation were suggested in view of a minimum-invasive laser dentistry [31].

Solving of the mathematical equations requires detailed input data on enamel's inhomogeneity and anisotropy. These structural properties result in additional complications associated to differences between cusps of the same tooth, as evidenced by SEM [32] and PIXE elemental analysis [33]. A noninvasive and convenient approach for the evaluation of enamel surface anisotropy could diagnose the orientation of prisms by reflectance measurement of optical constants [34], and such technique could provide valuable data for improving the models. However, there are relatively few previous experimental [9, 35, 36] and theoretical [29] studies on the influence of enamel surface anisotropy in laser irradiation.

*Aim*In a larger picture, the understanding of the possible physical mechanisms underlying the generation in enamel of periodic structures by laser irradiation, and their dependence on prisms orientation, appears as the main theoretical challenge of the present study. To this purpose and also for the other effects, we approach the interpretation of surface ultrastructure alterations observed by SEM and AFM in terms of ablation mechanisms. Both in Part II and Part III, physical concepts more close to experiment as compared to the above mentioned investigations are introduced and a deeper insight of the underlying physical processes is searched in terms of simple models beyond the descriptive SEM and AFM images of enamel.

To understand the origin of the short-wavelength RPS patterns seen by SEM in enamel with perpendicular prisms, interdependent electrodynamic and thermophysical mechanisms [2] are postulated in Part II. The energy balance of the interactions between the laser pulse and enamel are outlined.The dependence of the AFM-measured roughness vs. fluenceand the physical events produced at the surface layer of enamel associated to 10.6 μm pulses are discussed. For the sake of coherence, in the following the sequence of these issues will pursue approximately the reverse of their order in the above considerations.

Possible clinical implications of the detailed physical analysis based on all our theoretical models will be considered jointly in Part III.

2. Physical mechanisms and models of the effects of TEA CO_2 laser irradiation of dental enamel

Comments on the surface roughness vs. fluence relationship of the laser-irradiated enamel

In Part I of our study [1] we presented the ultrastructural effects of pulsed TEA-CO_2 laser ablation of dental enamel and cementum at nominal fluences of 75, 175 and 625 J/cm^2 as examined by SEM and AFM. Notable differences were seen in enamel with perpendicular and parallel prisms relative to the surface; they will be discussed later. The AFM data points representing the dependence on fluence σ of the RMS roughness R measured in square fields of 20 μm sides for the CO_2 laser irradiated enamel with perpendicular prisms are consistently fitted

above the fluence threshold σ_c with an exponential saturation curve or, alternately, with a Langmuir function which basically describes surface adsorption-desorption phenomena (Fig. 1):

$$R = \begin{cases} R_0 = const., \ for \ \sigma \le \sigma_c \\ R_0 + (R_{max} - R_0)\left[1 - \exp\left(-\frac{\sigma - \sigma_c}{s}\right)\right], \quad or \quad \frac{R_{max} b \sigma^{1-c}}{1+\sigma^{1-c}}, \ for \ \sigma > \sigma_c \end{cases} \tag{1}$$

In the exponential function R_0 is the roughness in the absence of laser irradiation, R_{max} is the maximum (saturation) roughness produced by laser, and s is a saturation constant with the dimension of fluence.

$$s = (\sigma_{1/2} - \sigma_c)/\ln 2 \tag{2}$$

$\sigma_{1/2}$ being defined as a 'half-fluence' producing a $(R_{max} - R_0)/2$ increase of roughness.

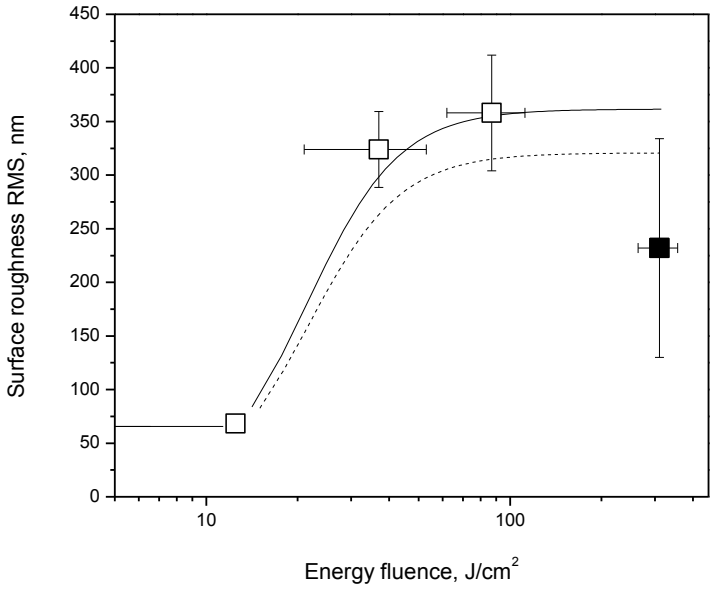

Fig. 1. The dependence of the AFM-measured RMS roughness on laser fluence for irradiated enamel with perpendicular prisms. Open squares and solid line, upper incisor with ordered prisms. Full square, lower molar with disordered prisms. The open and full squares were included together in the fit with the dashed line. The fit curves are Langmuir functions which are almost identical to the exponential saturation functions except the region near the fluence threshold (from about ~13 to ~30 J/cm^2).Thermal effects of successive ~2 μs laser pulses yielding a fluence of 25 J/cm^2 each were not overlapping with each other due to the long time (~10 s) between them

In the Langmuir function R_{max} has the same meaning as above while b and c are parameters. The Langmuir and exponential functions differ only for small values of the fluence σ above the fluence threshold σ_c. Here the exponential function behaves like σ while the Langmuir function behaves like σ^{α}, where α is a numerical constant ($\alpha \neq 1$).However, the experimental errors both in σ and in R were too large so as to distinguish between the two functions.

The exponential function is a solution of the differential equation:

$$\frac{dR}{d\sigma} = \frac{(R_{max} - R)}{s} \tag{3}$$

where the fluence σ is approximated as a continuous variable neglecting its stepwize increase with the number of pulses. By integration the constants of the exponential function (1) are found:

$$R_{max} = R(\sigma \to \infty) \tag{4a}$$

$$R_0 = R(0 \le \sigma \le \sigma_c) \tag{4b}$$

Thus towards infinite fluence (i.e., after an infinite number of laser pulses) the roughness approaches asymptotically a finite saturation roughness R_{max}.The differential equation (3)shows that the rate of roughness vs. fluence $dR/d\sigma$ is proportional to the difference between the saturation roughness R_{max} and the current roughness R. Moreover it shows that the more R approaches R_{max}, the smaller is the effect produced by a new laser pulse; or, put it in other words, the higher the already cumulated fluence, the smaller the change in roughness induced by a new pulse. The involvement of a saturation roughness R_{max} means that the surface layer melted by each laser pulse 'relaxes' subsequently by its own internal dynamics which opposes to the external action, arriving thus at a modified state less susceptible to change by a new laser pulse; so that in the end saturationis reached. This behavior is probably determined by the fact that the thermal effects of laser pulses were not overlapping due to the long time between them at the very low frequency used.

For a better understanding, a simple derivation of a Langmuir equation – formally identical to the derivation of the adsorption-desorption isotherm of a gas on a solid surface [37] – is at hand once the existence of a finite saturation roughness R_{max} is presumed. For convenience we define a fractional roughness θ:

$$\theta = \frac{R}{R_{max}} \tag{5}$$

which is produced by a fluence σ of the laser beam. Correspondingly the surface maintains a fractional non-alteration 1 – θ. The velocity of ablation during the action of the laser beam v_a is proportional to the fluence σ and to this fraction:

$$v_a = A\sigma(1-\theta) \tag{6}$$

After the pulse, the melted surface relaxes with a velocity v_r proportional to the fractional roughness θ already produced by the laser pulses and to a Boltzmann factor because the relaxation has to overcome an energy barrier ΔE:

$$v_a = B\theta \; exp\left(-\frac{\Delta E}{k_B T}\right) \tag{7}$$

Assuming that at equilibrium the speed of the two processes is equal, we get after simple calculations:

$$R = R_{max}\frac{b\sigma}{1+b\sigma} \tag{8}$$

where

$$b = \frac{A}{B} exp\left(+\frac{\Delta E}{k_B T}\right) \tag{9}$$

is a constant parameter for given irradiation conditions. If we also take into account the fluence threshold σ_c, eq. (8) takes the form:

$$R = R_{max}\frac{b(\sigma-\sigma_c)}{1+b(\sigma-\sigma_c)} \tag{10}$$

The Langmuir and the exponential saturation approaches lead to similar – but not identical – physical insight on the laser ablation of enamel. Thus the derivation of the Langmuir equation requires the *a priori* assumption of a finite saturation roughness R_{max}, just as for the exponential saturation equation; this is a remarkable similarity. However, in the derivation of the Langmuir equation an explicit thermal relaxation process with a specific energy barrier taking place in the melted enamel after the laser pulse is postulated from the beginning, while in the exponential saturation treatment such a process is remarked only *a posteriori*.

A critical fluence σ_c = 13 J/cm^2 was assumed (Fig. 1), a value where inhibition of caries-like lesions produced by *in vitro* demineralization was evidenced by use of sectioned enamel microradiography [38]. This value was a median between the threshold values where ultrastructural changes as seen by SEM (surface melting and crystal fusion) were reported to start, namely from 6.0 J/cm^2[18] or from 20 J/cm^2 [39], depending on the applied laser pulse sequences and on the methods used for assessing the changes. With a threshold of 13 J/cm^2, one finds $R_{max}\approx$ 360 nm for the upper central incissive alone and $R_{max}\approx$ 320 nm if the data of the incissive and of the lower molar are pooled and fitted together.

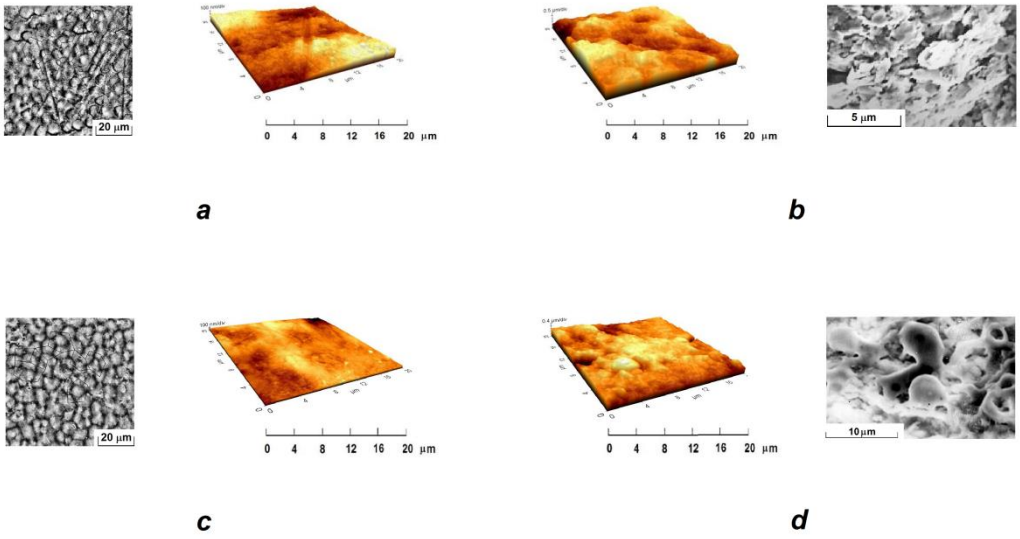

Fig. 2. SEM and AFM images of native (a, c) and irradiated (b, d) enamel with different structure and packing of perpendicular prisms. Prisms in the native enamel from upper incisor (a) have slightly smallar size and more regular packing as compared to the native prisms from the molar (c). Laser irradiation with a lower fluence of 175 J/cm^2 of the incisor enamel (b) produced effects of comparable magnitude as a fluence of 625 J/cm^2 on the molar incisor (d).

The significant decrease of the saturation roughness R_{max} occurring when the data of the molar was included in the fit suggests a different response of this tooth's enamel as compared to the incissive's enamel, although the prisms were perpendicular on surface in both teeth. Therefore it is plausible that besides the orientation of prisms, other structural factors, such as size and form of prisms, crystallinity and interprism enamel filling the volume between prisms, should play a role in the effects of laser irradiation. Presumably, the lower value of the molar's R_{max} may be due to the closer packing of prisms and lower fraction of interprism enamel and, together with a higher amount of prism enamel in the molar than in the incisor. Thus the same laser energy had to ablate more enamel in its hardest crystallized form at the surface layer of the molar and produce less effects. In other words, a higher fluence on the molar produced a similar roughness as a lower fluence on the incisor due to the enamel prism structure (Fig. 2).

The TEA-CO_2 laser action on enamel shows features related with other laser effects which present formally similar fluence dependencies with an initial lag and increase above a threshold

reaching saturation asymptotically. Analogous behaviour was shown by the ablation rate of enamel and dentin exposed to femto-and picosecond lasers [3, 6], by the CO_2 laser cut depth in bone [7,8], and by the ablation rate of non-biological materials with various hardness and melting point like ceramics, aluminum and steel [10]. These examples suggest that the laser action on enamel has a common nature with other laser ablation processes.

Also, there is an analogy of the enamel surface roughening produced by laser ablation with a surface absorption-desorption phenomenon as shown by the similar curve of the desorption yield of different ions ejected from dentin when irradiated with a free electron laser (FEL); the later increases above a threshold and then saturates [40]. Implicitly, this justifies the use of a Langmuir function in eq. (1) and in Fig. 1.

A partial likeliness is found with the relationships between fluence and a number of variables which characterize the generation of plasma on metallic targets [41]. The later include plasma onset time andthe quasi-unidimensional flowing thickness of the vapour-plasma mixture produced in the ablation of aluminum by a CO_2 laser; both vary fast above a threshold and, even if they did not reach saturation in the investigated fluence domain, the absolute values of their derivatives decreased monotously to a constant value, similarly to the terminal branches of our curves. This suggests that the RMS roughness vs. fluence effect may also involve a contribution related to the fluence dependence of plasma formation.

Interestingly, equations of precisely the same form as the exponential saturation describe the spatial dependence of the magnetic field component of surface electromagnetic waves induced by a light beam of parallel rays of wavelength λ which irradiates under angle θ a metallic surface covered with a wavy structure of period $\Lambda = \lambda/(1 - \sin\theta)$ forming a diffraction grating [42]. Note that in this case the condition $\Lambda \approx \lambda$ is fulfilled, just as for the resonant periodic structures observed in the irradiated enamel with perpendicular prisms, which will be discussed later.

The analysis shows that various possible factors may be involved in the asymptotic saturation of the RMS roughness vs. fluence dependence. The TEA-CO_2 laser ablation of enamel appears to be similar in essence with the pulsed laser ablation of other materials under certain conditions. Further studies are needed to understand better the mechanisms involved, surface phenomena of the absorption-desorption type, plasma formation/evolution and surface electromagnetic waves associated to diffraction on the resonant periodic structures with $\Lambda \approx \lambda$may bring their contribution to the 'relaxation' of the surface layer melted by each laser pulse – or to the negative feed-back by which the irradiated enamel opposes to the external action resulting in the asymptotic saturation of roughness for large values of fluence.

The analysis also suggests that every pulse produces ultrastructural [18, 38, 39] and chemical [18] changes in the enamel (e.g., by converting hydroxyapatite to acid phosphates and other compounds with higher melting and boiling point [16]) and probably crystallographic alterations, which in turn make more and more difficult the induction of further changes by subsequent pulses. Note however that while the morphology of changed enamel surface on the scale of tens of micrometers as observed by SEM ('waves' and bubbles) seems to be less reflecting and thus more absorbent of the laser IR radiation, the sealing of the surface defects on a micrometer scale as seen by AFM probably reduces the absorbance. These two possibly opposed trends illustrate the complexity of the laser–enamel interactions, discussed below.

Physical events and energy balance

A physical discussion of the laser beam–enamel interactions may contribute to a better understanding of the observed modifications of the surface morphology. The laser ablation mechanisms and interactions were extensively studied in non-biological materials [2, 43 – 45] and biological tissues [5, 46] including teeth [4, 11, 26]. The effects produced by the pulsed 10.6 μm laser radiation on the dental enamel and cementum described in Part I [1] were very complex. The efficiency of CO_2 laser is due to the fact that its wavelength overlaps almost perfectly to the most intense absorption band due to symmetric (ν_1) and antisymmetric (ν_3) phosphate P-O bond stretching around 1000 cm^{-1}.

A nominal average fluence of 25 J/cm^2 was used for each pulse, a value which was well above the threshold of 13 J/cm^2 where the first ultrastructural changes appear and equal to the level where macroscopic effects begin to appear [38]. But the effective energy fluence involved in the observed surface morphology changes was much lower due to various losses occurring during the laser action.

A small amount of the incident radiation is reflected directly by the tooth surface, probably not exceeding 5% as in the case of other biological tissues [46]. Of the remaining beam which enters in the hard tissue a somewhat larger fraction is scattered, and finally the rest undergoes absorption. The attenuation process is described by the well-known Lambert-Beer law. For a beam of incident intensity I_o and emerging with an intensity I after crossing a layer of thickness z it writes:

$$I = I_o \exp[-(\mu_a + \mu_s)\, z] \tag{11}$$

where μ_a and μ_s are the absorption and scattering coefficients which determine the relative emerging intensities of the two components by the corresponding factors $\exp(-\mu_a z)$ and $\exp(-\mu_s z)$.More generally, for an unpolarized laser beam with Gaussian profile which undergoes reflection, scattering and absorption in the target, the intensity at distance r from the centre of the spot and at depth z from the surface is given by (e.g., [47]):

$$I(z,r) = I_0(1-R)F_{sc}\, exp[-(\mu_a + \mu_s)z]\; exp\left(-\frac{2r^2}{w^2}\right) \tag{12}$$

Here,$w$is the beam radius,I_0 is the intensity of radiation at the centre of the laser spot, R is the Fresnel reflection coefficient for unpolarized light, and F_{sc} accounts for the scattering. However in the following a rough approximation by the simple eq. (11) is sufficient.

A fraction of the absorbed CO_2 laser radiation is involved in a multiphoton excitation of vibrational levels which induces a visible emission of dental enamel at a photon energy of 2.07 eV [48]. The IR induced visible luminiscence cannot be described by radiation heating of the sample. The visible radiation can be detected in a narrow resonant frequency range which corresponds to vibrational excitation in the stretch mode of the PO_4 ion in carbonated hydroxyapatite (HA) around ν_3 = 1088 cm^{-1}. Under a high-fluence IR pulse a considerable fraction of vibrational excited PO_4 groups can pass to an excited electronic state which allows for the emission of visible light.

The absorbed and scattered fractions may be approximately estimated from the IR spectra of HA, the main component of dental enamel and other hard tissues of teeth. In the IR spectrometry of inhomogeneous solids, the coefficients μ_a and μ_s cannot be rigorously evaluated, because they depend on the sample characteristics (composition, structure, crystallinity, anisotropy, thickness ordensity) and, therefore, the spectra are given in terms of percent transmittance, defined in general as $T = I/I_o$. From HA spectra one can find the transmittance $T_s$of a layer of thickness z in regions (e.g. 2000 cm^{-1}) where practically all attenuation is due to scattering and no absorption takes place, while the transmittance is $T_{a+s} = T_a T_s$ for the strong absorption band of around 1000 cm^{-1}. As the scattering varies slowly within the considered domain, we assume it to be roughly constant, and thus the weights of absorbed and scattered intensities can be evaluated. From the IR spectra of a pure HA sample [49] and of dental enamel [50], by supposing 5% reflection, we evaluated fractions of 82 – 88% absorbed radiation and of 7 – 13% scattered light. Of the later, only a part is backscattered while the remaining is scattered inside the surface layer and is eventually absorbed by the enamel contributing to the laser radiation effects.This does not change much the balance. Making use of the fraction of absorbed radiation and of Lambert-Beer law one can evaluate the product $\mu_a z$ and hence, by assuming pathlengths of 50 to 100 μm, a mean absorption coefficient of 340 ± 120 cm^{-1} is guessed for the 10.6 μm radiation in HA (and enamel), that is, about 1/3 of the water value. In fact the tissue component that maximally absorbs CO_2 wavelength is water followed by apatite [51]. The penetration depth d, defined as the depth at which the collimated beam is attenuated by factor 1/e(37%)

$$d = \frac{1}{\mu_a} \tag{13}$$

is thus estimated in enamel to be of about 20 – 40 μm. From eq. (11) one finds a value of 90 – 180 μm for the depth z_{99} where 99% of the non-reflected and non-scattered radiation is absorbed and practically all its energy is deposited in the enamel surface layer. This result is in agreement with the laser-affected depth experimentallydetermined in enamel for similar fluences per pulse. Using a fluence per pulse of 2.6 J/cm^2 and a total fluence up to 50 J/cm^2, a depth of 10 μm was estimated [38]; with pulses of 0.3 J/cm^2 summing a 610 J/cm^2 total fluence the depth was of 12 μm [52]. A considerably larger depth, but not exceeding 100 μm is to be expected for a fluence per pulse of 25 J/cm^2 and total fluence of 625 J/cm^2. In general, for materials with high absorption coefficient (>100 cm^{-1}), the confined absorption and action of pulsed CO_2 laser radiation takes place within about 100 μm [53]. It applies for isolated pulses delivered at low rate as in our experiment, allowing the irradiated enamel layer to come back close to its initial temperature before the next pulse is arriving. While we estimated an order of magnitude for the depth of the affected layer, its precise value obviously depends on the particular surface structure of the enamel, e.g. on the orientation of enamel prisms (see Fig. 4 below).

The 80 – 90% absorbed energy (4.0 – 4.5 J) of the incident laser beam triggers a very fast sequence of events leading to temperature jumps of thousands of degrees within the ~2 μs duration of the laser pulse of about MW power. However, not all absorbed energy is used for melting and ablation of enamel resulting in the observed surface morphology changes; in the case of the TEA-CO_2 laser, about a half is lost in the plasma generation.

Various changes produced by heating in enamel have been reviewed [5, 11, 26]. An appreciable but relatively not important fraction of laser energy was used for changing the chemical composition of enamel. The rate of decrease in concentration of a chemical component of the target $D(t)$ is assumed to change with temperature $T(t)$ according to the Bolzmann statistics.The hard tissue chemical damage, i.e. decrease in molecular component $D(\tau)$, relative to its initial value D_0 over the pulse duration τ, is given by the integral Ωof the Arrhenius equation [54, 55]:

$$\Omega(\tau) = -ln\left(\frac{D(\tau)}{D_0}\right) = A\int_0^{\tau} exp\left(-\frac{E^*}{RT(t)}\right)dt \tag{14}$$

Here,E^* and A are the activation energy and rate constant parameters of the process,τis the upper integration limit,and R is the gas constant, 8.3 J/(K·mol). This amount depends onT(t), the time evolution of the temperature during the laser pulse;chemical effects extending in the cooling phase after the pulse are neglected.

The process starts by sudden evaporation of the small amount of water above 100 ^oC and by partial photocarbonization of the organic components (collagen, keratin, citrate) up to 400 ^oC; however, small energy is lost in this process because these two components together average only 4% of the total. Note that the decomposition of the organic matrix of enamel decreases the ion diffusion and reduces enamel demineralization. Between 100 and 1100 ^oC carbonate loss occurs, which diminishes enamel solubility. Crystallographic changes and conversion of acid phosphate to pyrophosphate take place from 100 to 650 ^oC and further up to 1100 ^oC when less soluble compounds are forming. However from 1100 ^oC on more soluble crystalline phases are produced. Generally, from 300 ^oC up to the melting point of enamel at 1280 ^oC [56], the hydroxyapatite changes chemical structure to minor phases represented by other phosphates which, together with the native hydroxyapatite, form a mixture, with a melting point of about 1600 ^oC [50]. Depending on temperature, these changes influence the enamel resistance to demineralization.

The heating by $1/e^2$ (Gaussian) spot is not uniform, and the fluence of 625 J/cm^{2}produced boiling of melted enamel in the centre and concentric waves in the outer region as described in Part I and discussed subsequently in Part III. Thuswe suppose the temperature was significantly higher than 1600 ^{o}C in the centre and appreciably lower at the spot boundary. Moreover the local temperature in the spot would be approximately proportional to the scalar heat flux density, which in turn would scale roughly like the absorbed fraction of the radiative flux density (irradiance). All these quantities are measured in W/cm^2 and would probably show a more or less Gaussian profile in the laser spot. Accordingly, the crystallographic and chemical changes should show also a radial gradient, and the depth of the melted enamel layer should be larger at the centrum as compared to the outer regions.

As already mentioned, other important energy losses are due to the plasma induced by laser irradiation. This aspect will be treated in Part III.

Resonant periodic structures in enamel with perpendicular prisms. Electrodynamic approach

The enamel with perpendicular prisms of the lower molar irradiated with pulses of Gaussian profile from the TEA-CO_2 laser at 625 J/cm^2 fluence evidenced two periodic patterns, one with a longer period of ~42 μm, and a second wavy structure with a shorter period of 11.0 ± 1.5 μm, but not always superimposed on the former (Fig. 3A and 3B, respectively). The qualitative analysis of Part I showed that the 11.0 μm frozen waves meet at least two characteristics of RPS which emerge due to diffraction and interference of laser radiation in the sample surface layer. First and most important, their ~11.0 μm period is close to the 10.6 μm wavelength of laser radiation, $\Lambda \approx \lambda$. Second, the formation of RPS is favored by the presence of defects on the irradiated surface [2], and in fact the 11.0 μm waves were observed only on the irradiated enamel with perpendicular prisms which had the larger surface density of defects. The formation of RPS was demonstrated since long in metals (reviews in [2, 45]), fused silica, inorganic crystals [68, 69] and in metallic nitride ceramic multilayered coatings [70]. Our observations are remarkable not only because they provided the first evidence of wave-like patterns produced by laser irradiation in dental enamel and in biological tissues in general, but also because we evidencedfor the first time in a calcified tissue resonant periodic structures, confirming therefore their "universal" nature [70]. It is worth noting that in the inorganic targets, either conductive or insulating but with a more regular structure, the RPS were induced by very short laser pulses (from nano- to femtoseconds), while in the electroinsulating dental enamel with a complex, hierarchical, anisotropic, inhomogeneous and apparently less ordered spatial structure they were generated by the much longer nanosecond pulses of the TEA-CO_2 laser, whose wave-generating action proved to be independent of the enamel's structural characteristics.Because the laser radiation was unpolarized, it is not yet clear why the crests of the waves were oriented within less than $\pm 30^o$ about a preferential direction. It is currently admitted that the RPS arise by complex, non-singular, interdependent mechanisms, both electrodynamic and thermophysical, which are not yet fully understood (review in [2]). We first consider the electrodynamic side of the problem.

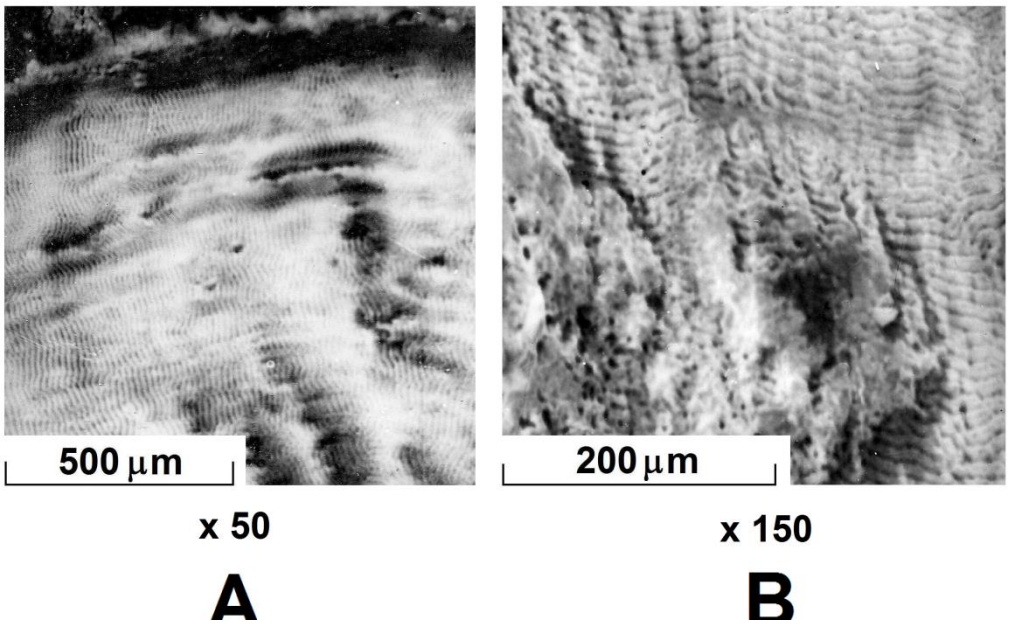

Fig. 3. Resonant periodic structures of 11.0 ± 1.5 μm superimposed (A) and not superimposed (B) on non-resonant peridic structures of ~42 μm, produced by the TEA-CO_2 laser radiation at 625 J/cm^{2}fluence on the surface of enamel with perpendicular prisms of the lower molar. The crestes of the RPS were oriented within less than $\pm 30^o$ about a preferential direction.

The RPS was generated on enamel surface by unpolarized radiation focused on the target. A parallel beam of 2 cm emerging from the CO_2 laser source was focalized in a 0.5 cm spot on the tooth placed at 5 cm from the AR germanium lens. The angle between the radiation and the normal to the surface varied therefore between 0 and 8.5^o. The theory allows for calculations the RPS period Λ as a function of wavelength λ and angle θ in the case of oblique incidence of linearly polarized radiation [2]. If the radiation is polarized in the incidence plane, we have:

$$\Lambda = \Lambda_{\parallel} = \frac{\lambda}{1 - \sin\theta} \tag{15}$$

while in the case of radiation polarized perpendicular to the incidence plane the period is:

$$\Lambda = \Lambda_{\perp} = \frac{\lambda}{\cos\theta} \tag{16}$$

In our experiment with focalized and unpolarized radiation, each contribution has to be integrated over θ which varies between 0 and a maximum value because the beam is focused, which is characterisedby angle-averaged values of:

$$\overline{\Lambda_{\parallel}} = \frac{\lambda}{\theta_{max} - 0}\int_0^{\theta_{max}} \frac{\lambda}{1 - \sin\theta}\, d\theta \tag{17}$$

$$\overline{\Lambda_{\perp}} = \frac{\lambda}{\theta_{max} - 0}\int_0^{\theta_{max}} \frac{\lambda}{\cos\theta}\, d\theta \tag{18}$$

The parallel angle-averaged value (11.48 μm) derived from the $\Lambda = \lambda/(1 - \sin\theta)$ assumption gives a more important contribution to the observed period of 11.0 μm than the perpendicular angle-averaged value (10.64 μm) which remains close to the radiation wavelength of 10.6 μm. To describe the RMS wavelength of the RPS produced by irradiation with unpolarized radiation, one has to take some mean value of the above angle-averaged values estimated for parallel and perpendicular polarization, such as the arithmetic mean, the geometric mean, the root mean square

$$\langle \Lambda_{\mathrm{RMS}} \rangle = \sqrt{\left(\overline{\Lambda_{\parallel}^2} + \overline{\Lambda_{\perp}^2}\right)/2} \tag{19}$$

or the integral mean over the effects produced by radiation along the two main directions of polarization:

$$\langle \Lambda_{\mathrm{Int}} \rangle = \frac{\lambda}{\theta_{max} - 0}\int_0^{\theta_{max}} \frac{\lambda}{(1 - \sin\theta)\cos\theta}\, d\theta \tag{20}$$

To compare with the experimental value $\Lambda = 11.0 \pm 1.5$ μm, we introduce everywhere $\theta_{max} = 8.5^{o} = 0.1483$ rad and, because one does not know the mean values which corresponds better to the real situation of unpolarized radiation, we take the mean of the means and we get $\langle\Lambda\rangle = 11.13 \pm 0.14$ μm. On the other hand, for the similarly estimated, physically determined limits of the RPS we get $\Lambda = 10.6 \div 11.84$ (±0.50) μm. Thus the calculated values are in excellent agreement with the experiment and the theory confirms that the short period frozen waves have the characteristics of a diffraction grating and are indeed RPS produced by the interference of the incident and scattered radiation from the melted enamel layer. As already mentioned, the same diffraction grating characteristic of the RPS approximately described by the equation $\Lambda \approx \lambda/(1 - \sin\theta)$ and persisting beyond the laser pulse duration, may be related somehow to the exponential saturation describing the spatial dependence of the magnetic field component of surface electromagnetic waves induced by the light beam [2, 42].This has the same form as the observed exponential saturation of the RMS roughness dependence on fluence for the CO_2 laser irradiated enamel with perpendicular prisms.

Note that the RPS were observed only after 25 laser pulses (625 J/cm^2) and not when 7 or 3 pulses were applied. In fact the relief growing on the surface sharpens with the increase in the number of pulses [2]. Also, they seem to follow not any preexisting defects, e.g. the boundaries of the enamel prisms as they were oriented within less than ±30^{o}around a preferential direction (Fig. 3). Thus the formation of RPS starts from preexiting defects and their initial pattern follows the later when produced by a single laser pulse, but in the case of multipulse laser irradiation the initial pattern is wiped out and a linear pattern with a dominant direction results [2].

A diversity of electrodynamic mechanisms for RPS formation were proposed. A positive feedback mechanism was suggested [71] by which the RPS grow out of the random noise of space harmonics of the surface roughness by forming on the melted surface layer a grating with $\Lambda \approx \lambda/(1 - \sin\theta)$ which directs the light wave diffracted in -1 order into the material; in turn, this wave interferes with the refracted beam and creates an intensity grating of the same period Λ but shifted by a phase difference Φ as compared to the initial grating. The non-uniform absorption of energy was also accounted by the interference of the refracted wave with the electric field of a periodic dipole layer forming at the surface of the target [2]. Other authors suppose that the modification of

the surface ultrastructure is the result of the action of electromagnetic fields generated on the surface roughness by interference of incident and scattered waves [72, 73]. Attempts have been made to explain the RPS by spatial modulation of the complex dielectric permittivity due to surface effects of the refraction index n and of the extinction coefficient k ($\varepsilon_c = |n + ik|^2$); these effects and not surface roughness were assumed to be responsible for modulating the scattering of radiation [71, 74]. The feedback mechanisms allows the calculation of the increase or damping in time of the relief amplitude [2], an aspect which may be related to the exponential saturation of the AFM-measured RMS roughness as a function of fluence.

The profile of the RPS can be described by a sinusoid:

$$z(x) = h\ \cos\frac{2\pi x}{\Lambda} \tag{21}$$

where h is the relief depth or amplitude, which was found to be of 0.1 – 0.4 μm for various metals irradiated with 10.6 μm, that is about 1 – 4 % of Λ [2]. However, in the case of ceramic multilayered coatings irradiated by laser light of 775 nm,h amounted to 47 % of Λ [70]. For the electroinsulating enamel we could therefore expect a h/Λ ratio above 10 percent. An expression has been derived for the relief depth [2]:

$$h = h_o = \frac{\Lambda}{2\,\pi}\sqrt{A_o \cos\theta} \tag{22}$$

where A_o is the absorptivity of the unirradiated plane surface. For the hydroxyapatite which is the main component of enamel the absorptivity of 10.6 μm radiation is high, evaluated above to 82 – 88 %, and for the irradiation geometry used $\cos\theta \geq 0.98892$. Thus for Λ = 11.0 μm we have $h \geq$ 1.58 μm and $h/\Lambda \geq$ 14.3 %. The formation of RPS influences the optical properties of the surface and in particular the actual absorptivity A of radiation which can strongly increase, even to 100 % [2]; however in the case of enamel this increase probably is not very spectacular given the high initial absorptivity A_o.

The electrodynamic approach evidences a spot diameter dependence of the efficiency of energy conversion of induced surface electromagnetic waves inside and outside the spot. From a practical viewpoint the achievement of the 'large' irradiation spot condition allows almost all the incident energy to be absorbed by the rippled surface [2]. However the diameter x_o of the large spot is governed by the relation $\alpha x_o \gg 1$, where α is the attenuation coefficient of surface electromagnetic waves, and depends of the material; for insulators $x_o$can be inferiorto 1 mm. Also, the total absorptivity A is larger when the $\boldsymbol{E}$ vector of the linearly polarized incident wave is directed along the longest side of the target. Further studies may help to take advantage of these two behaviors for optimizing the irradiation conditions of teeth according to the desired practical effects by taking into account the anatomical shape and size of the tooth.

Finally let us mention that the electrodynamic treatment of RPS formation is not sufficient and that it describes only one side of the problem; the other one is inseparably related to the thermophysical part of the phenomenon discussed further.

Resonant periodic structures in enamel with perpendicular prisms. Thermophysical approach

A correlated examination of the electrodynamical and thermophysical mechanismsimplied in the RPS generation involves the following steps [2]: 1) the determination of the radiation field generated inside the surface layer as a result of interference between the incident and diffracted waves; this field determines the spatial distribution of the power density of the heat source; and 2)

the determination of the spatial distribution of temperature which nextcontrols the induction of forces modifying the surface relief and thus the radiation field by a feedback chain.

Various mechanisms have been proposed for the second stage. In the model of surface acoustic waves one has to solve the vector equation of elastic deformation of the medium. Capillary waves on molten surface layer are solutions of the hydrodynamic equations [75]. In this case RPS form due to the temperature dependence of the surface tension. It is postulated that RPS depressionis more strongly heated than the crests and the molten substance is evacuated from the depression, where the superficial tension is lower than on the crests, and thus the RPS are further sharpened by a positive feedback [2]. In the mechanism of interferential instability the equation of displacement of the vaporization front is used [75 – 77]. In the mechanism of the RPS generation by vaporization and neglecting the melt removal under the action of a reactive recoil pulse of vapor, the threshold of laser pulse fluence for the growth of RPS in large irradiation spots is given by:

$$E_s^p = \frac{\rho q \Lambda}{8\pi} \tag{23}$$

where ρ is the density of the material and q is the specific heat of vaporization. This relation requires for the laser pulse duration τ the accomplishment of the condition:

$$\tau_L \ll \frac{\lambda^2}{4\kappa} < \frac{\Lambda^2}{4\kappa} \tag{24}$$

Here κ is the thermal diffusivity of the target substance. Because one has no access to an accurate value of κ in enamel, we made a crude estimate by assuming κ to be roughly the same in enamel and bone and by referring to a formally similar relationship which helped evaluate the thermal response time constant in bone ($\tau_T \sim 25$ μs).Hence one can infer a characteristic length equal to the penetration depth, $\delta \approx d = 1/\mu_a, \approx 20 – 40$ μm. Thus for $\Lambda = 11.0$ μm, one gets $\Lambda^2/4\kappa = 2 – 7.5$ μs. For the enamel irradiated with the $\tau = 2$ μs pulses of the TEA-CO_2 laser, the condition (24) seems therefore to be 'softened' to $\tau \leq \Lambda^2/4\kappa$ instead of $\tau \ll \Lambda^2/4\kappa$. This suggests that the irradiation was performed at the *limit* of eq. (24) domain of validity, *i.e.* close to and slightly above the threshold of laser pulse fluence required for the morphogenesis of the RPS. This result is consistent with the experimental evidence.

In Part IIIa simple thermophysical model is introduced, aiming to describe in a similar way both the resonant and non-resonant periodic structures.

3. Conclusions

In agreement with the experimental data, the equations which describe the AFM-measured RMS roughness vs. fluence relationship show that the laser-enamel interaction is characterized by a saturation roughness R_{max}. This resulted by the competition between the laser pulse melting of the surface layer and its 'relaxation' by own internal dynamics which opposes to the external action.Ithas to overcome a material-dependent energy barrier.

With reasonable assumptions, the energy balance of the phenomena involved in the interactions between the laser pulse and enamel were outlined.Noteworthy, a large amount of the incident energy is lost in the plasma, but this will be discussed in Part III.

Theoretical models were proposed in order to explain one of the most remarkable characteristics of the ablation patterns produced by the pulsed TEA-CO_2 non-polarized Gaussian laser beams at 625 J/cm^2 fluence: the resonant periodic structuresof ~11 μm period imprinted on the surfaceof enamel with perpendicular prisms.The experimentally-measured period Λ of the RPS

could be compared with theoretical values determined as a function of wavelength λ and incidence angle θ in the frame of the electrodynamic approach. In our experiment with focused and unpolarized radiation, each contribution has to be integrated over θ which varies from 0 to a value θ_{max} = 8.5^o characteristic to the experimental arrangement, giving thus angle-averaged values, estimated for parallel and perpendicular polarization. Taking then the arithmetic mean, the geometric mean, the root mean square of the later and finally the average of the means we found ‹Λ› = 11.13 ± 0.14 μm, which compares excellently with the experimental value Λ = 11.0 ± 1.5 μm. Therefore the electrodynamic theory demonstrates diffraction grating properties of the short period waves and thus their RPS nature was confirmed beyond any doubt; accordingly, they were produced by the interference of the incident beam and radiation scattered from the melted enamel layer. Moreover, taking into account the values of Λ and of the absorptivity of hydroxyapatite at 10.6 μm, the relief depth or amplitude of the RPS has been evaluated to be of about 1.6 μm or ~15 % of the period. The proposed electrodynamic mechanisms for the RPS formation helped to reach a better understanding of the observed ultrastructural changes induced on enamel's surface.

However, the involved thermophysical phenomena are an inseparable part in the description of the process and provides a relevant insight of RPS growth. Thus by assuming that the RPS generation took place by vaporization only, the threshold of laser pulse fluence for the formation of the Λ ~ 11 μm waves in large irradiation spots is proportional to Λ itself and to the density and specific vaporization heat of the enamel.Also if the thermal diffusivity of the enamel is admitted to be roughly the same as for bone, it follows that for the 2 μs pulses of the TEA-CO_2 laser the irradiation was carried out in a limiting regime, close to and slightly above the threshold of laser pulse fluence required for the morphogenesis of the RPS.

The present results of the theoretical analysis encourage further development along this line for a better understanding of the other effects produced by the pulsed TEA-CO_2 laser irradiation research.They constitute the object of Part III of our study.

Acknowledgement

E.A.P. is grateful to Prof. Marian Apostol (Bucharest) for carefully reading the manuscript, detailed discussions and valuable suggestions in the development of the theoretical models. The authors express their sincere regrets for the disappearance of their colleague I. Patru, departed before the preparation of this article and keep a warm remebrance of his team work.

The authors acknowledge with thanks the partial support of this work by UEFISCDI under the contract 19_RO-FR/2014.

References

[1] E.A. Preoteasa, Elena S. Preoteasa, I.N. Mihailescu, P. Lucuta, A. Moldovan, Digest J. Nanomater. Biostruct. **8**, 987 (2013)
[2] A.M. Prokhorov, V.I. Konov, I. Ursu, I.N. Mlhailescu, Laser Heating of Metals, Adam Hilger, Bristol-Philadelphia-New York (1990)
[3] J. Neev, J. Squier, in Applications of Ultrashort-Pulse Lasers in Medicine and Biology, (J. Neev, editor), SPIE Proc. **3255**, 105 (1998)
[4] M. H. Niemz, Appl. Phys. B **58,** 493 (1994)
[5] M.H.Niemz, Laser-Tissue Interactions: Fundamentals and Applications, Springer-Verlag, Berlin Heidelberg New York (1996)
[6] M.H. Niemz, in Applications of Ultrashort-Pulse Lasers in Medicine and Biology, (J. Neev, editor), SPIE Proc. **3255**, 84 (1998)
[7] M.M. Ivanenko, P. Hering, in Thermal Therapy, Laser Welding and Tissue Interaction, SPIE Proc. **3565**, 110 (1998)
[8] M.M. Ivanenko, T. Mitra, P. Hering, Optical Biopsy and Tissue Optics,SPIE Proc. **4161-08**, 46 (2000)

[9] M.K. Yamada, M. Uo, S. Ohkawa, T. Akasaka, F. Watari, Mater. Transact. **45**, 1033 (2004)
[10] S.V. Garnov, V.I. Konov, T. Kononenko, V.P. Pashinin, M.N. Sinyavsky, Laser Phys. **14**, 910 (2004)
[11] P.A. Ana, L. Bachmann, D.M. Zezell, Laser Phys.**16**, 865 (2006)
[12] D. Fried, T.M. Breunig, Lasers in Dentistry VII, **4249**, 99 (2001)
[13] K. Nagai, J.-I. Kinoshita, Y. Kimura, K. Matsumoto. J. Oral Laser Applic.**6**, 265 (2006)
[14] S. Kantola, E. Laine, T. Tarna, Acta Odontol. Scand.**31**, 369 (1973).
[15] J. H. Meurman, J. C. Voegel, R. Rauhamaa-Mäkinen, P. Gasser, J.M. Thomann, J. Hemmerle, M. Luomanen, I. Paunio, R.M. Frank, Caries Res.**26**, 77 (1992).
[16] B.O. Fowler and S. Kuroda, Calcif. Tissue Int. **38**, 197 (1986).
[17] D.G.A. Nelson, J.S. Wefel, W.L. Jongebloed, J. Featherstone, Caries Res; **21**, 411 (1987)
[18] C. Steiner-Oliveira, L.K.A. Rodrigues, L.E.S. Soares, A.A. Martin, D.M. Zezell, M. Nobre-Dos-Santos, Dental Mater. J. **25**, 455 (2006)
[19] A. Sagi, T. Segal, J. Dagan, Math. Biosci. **71**, 1 (1984)
[20] G. Macaveiu, ISRN Biomed. Engn., Article ID 464293, (2013)
[21] D. Găzdaru, C. Chilom, M.A. Călin, C. Geantă, A. Popescu,Romanian J. Biophys. **18**, 73 (2008)
[22] L.V. Zhigilei, A.M. Dongare, CMES **3**, 539 (2002)
[23] M.E. Abadi, M.H. Miran Baygi, A. Mahloojifar, S. Moghimi, Iranian J. Electric. Electron. Engn. **1**, 23 (2005)
[24] T. Perhavec, J. Diaci, J. Laser Health Acad.**2(**1), 1 (2009)
[25] M.A. Golshan, M.G. Tarei, M.A. Ansari, A. Amjadi, J. Lasers Med. Sci. **2**, 109 (2011)
[26] D.M. Zezell, P.A. Ana, T.M. Pereira, P.R. Correa, W. Velloso Jr., 227-246 in: Developments in Heat Transfer (M.A. dos Santos Bernardes, editor), Published by InTech, Rijeka, Croatia (2011)
[27] M. Petrus, D.C. Dumitras, U.P.B. Sci. Bull., **A 74**, 167 (2012)
[28] M. Jaunich, S. Raje, K. Kim, K. Mitra, Z. Guo, Int. J. Heat Mass Transfer **51**, 5511 (2008)
[29] S.L. Jaques, S.A. Prahl, Laser Surg. Med.**6**, 494 (1987)
[30] M. Gantri, H. Trabelsi, E. Sediki, R. Ben Salah, J. Biophys. Article ID 253763, (2010)
[31] A. Vila Verde, M.M.D. Ramos, A.M. Stoneham,Phys. Med. Biol. **52**, 2703 (2007)
[32] T. Zeygerson, P. Smith, R. Haydenblit, Arch. Oral Biol. **45**, 1091 (2000)
[33] E.A. Preoteasa,Elena S. Preoteasa, A. Kuczumow, D. Gurban, L. Harangus, D. Grambole, F. Herrmann, X-Ray Spectrom. **37**, 517 (2008)
[34] G. Duplain, R. Boulay, P.A. Bélanger, Appl. Optics **26**, 4447 (1987)
[35] J.M. Ferreira, J. Palamara, P.P. Phakey, W.A. Rachinger, H.J. Orams, Arch. Oral. Biol. **34**, 551 (1989)
[36] S.M. Nomelini, A.E. Souza-Gabriel, M.A. Marchesan, M.D. Sousa-Neto, Y.T. Silva-Sousa, Microsc. Res. Tech. **72**, 737 (2009)
[37] E. Chifu, Coloidal Chemistry, Didactical and Paedagogical Publishing House [in Romanian], Bucharest (1969)
[38] R.H. Stern, J. Vahl, R.F. Sognnaes, J. Dent. Res. **51**, 455 (1972)
[39] S.M. McCormack, D. Fried, J.D.B. Featherstone, R.E. Glena, W. Seka, J. Dent. Res. **74**, 1702 (1995)
[40] S. Ogino, K. Awazu. Nucl. Instrum. Meth. Phys. Res. **B 144**, 236 (1998)
[41] M. Stoica, D. Craciun, I.N. Mihailescu, 136-151 in: Laser Research and Engineering (V. Vasiliu, editor), Central Institute of Physics, Bucharest-Magurele (1989)
[42] V.I. Emel'yanov, V.N. Seminogov; Kvantov. Elektron. (Sov. J. Quant. Electron.) **11**, 871 (1984)
[43] A.L. McKenzie, Phys. Med. Biol. **35**, 1175 (1990)
[44] A.A. Oraevsky, R.O. Esnaliev, V.S. Letokhov, 112-122, in Laser Ablation – Mechanisms and Applications (J.C. Miller, R.F. Haglund Jr., editors), Springer Verlag, Berlin-Heidelberg New York (1991)
[45] I. Ursu, IN Mihailescu, AM Prokhorov, VI Konov. Interaction of Laser Radiaton with Metals, Romanian Academy, Bucharest (1986)
[46] A.J. Welch, J.H. Torres, W.-F. Cheong, Texas Heart Inst. J. **16**, 141 (1989)

[47] M. Cutroneo, L. Torrisi, C. Scolaro, Laser applications in bio-medical field, Univ.Messina, Preprint (2012)
[48] A. Lohner, S.D. Ganichev, W.M. Huber, J. Diener, W. Prettl, Infrared Phys. Technol. **39**, 23 (1998)
[49] V. Geetha, G. Buvaneswari,Mater. Res. Bull.**45**, 1866 (2010)
[50] S. Kuroda, B.O. Fowler, Calcif. Tissue Int. **36**, 361 (1984)
[51] S. Gouw-Soares, A. Stabholz, J.L. Lage-Marques, D.M. Zezell, E.B. Groth, C.P. Eduardo, J. Clin. Laser Med. Surg. **22**, 129 (2004)
[52] K.M. Ramalho, Prevention of enamel erosion through CO2 laser irradiation. An in situ study,Thesis, Technischen Hochschule Aachen, Germany (2010)
[53] S. Zhang, CO2 Laser induced structural changes of dental enamel, Thesis, Univ. of Hamburg, Germany (2008)
[54] L. Pauling, General Chemistry, Third edition, W.H. Freeman Co., San Francisco (1970)
[55] Topcon Corp., Endpoint management: Advanced algorithms for controlled laser treatments, Tokyo (2012)
[56] D. Brune, Scand. J. Dent. Res. **88**, 301 (1980)
[57] I. Ursu, I. Apostol, D. Barbulescu, V. Lupei, I.N. Mihailescu, A. Popa, A.M. Prokhorov, N. I. Chapliev, V.I. Konov, Proc. SPIE Int. Soc. Opt. Eng. **398**, 361 (1983)
[58] V.A. Danilychev, V.D. Zvorykin, I.V. Kholin, A.Yu. Chugunov, Sov. J. Quantum El. **10**, 1518 (1980)
[59] V.I. Konov, Yu.V. Lavrent'ev, Yu.I. Stepanov, N.I. Chapliev, A.V. Shirkov, Sov. J. Quantum El.**13**, 1128 (1983)
[60] P. Viraparia, J.M. White, R.M. Vaderhobli, In: CO2 Laser - Optimisation and Application, (D.C. Dumitras, editor) InTech, Rijeka (Croatia)-New York-Shanghai (2012)
[61] V.I. Bergel'son, A.P. Golub', I.V. Nemchinov, S.P. Popov, Sov. J. Quantum El. **3**, 288 (1974)
[62] J.C. Koo, J. Appl. Phys. **48**, 618 (1977)
[63] B. Payne, The role of chromophore on pulsed laser ablation of biological tissues. Thesis, Univ. Denver (1994)
[64] C.T.E. Gordon Jr., J. Dent. Res. **45**, 372 (1966)
[65] A.G. Doukas, A.D. Zweig, J.K. Frisoli, R. Birngruber, T.F. Deutsch, Appl. Phys. **B53**, 237 (1991)
[66] J.P. Cummings, J.T. Walsh Jr., Appl. Optics **32**, 494 (1993)
[67] A.P. Alloncle, D. Dufresne, M. Autric, J. Physique IV, Coll. C4, Supp. 111, **4**, C4 (1994)
[68] P.A. Temple, M.J. Soileau, IEEE J. Quant. Electron. **QE-17**, 2067 (1981)
[69] F. Keilmann, Y.H. Bai, Appl. Phys. **A 29**, 9 (1982)
[70] B. Gakovic, C. Radu, M. Zamfirescu, B. Radak, M. Trtica, S. Petrovic, P. Panjan, C. Ristoscu, I.N. Mihailescu, F. Zupanic, Surf. Coat. Technol. **206**, 411 (2011)
[71] G. Zhou, P.M. Foucet, A.E. Siegman, Phys. Rev. **B 21**, 5366 (1982)
[72] J.F. Young, J.E. Sipe, J.S. Preston, H.M. van Driel, Appl. Phys. Lett. **41**, 261 (1982)
[73] A.M. Prokhorov, A.S. Svakhin, V.A. Sichugov, A.V. Tischenko, A.A. Hakimov, Kvantov. Elektron. (Sov. J. Quant. Electron.) **10**, 906 (1983)
[74] I.A. Avrutskii, P.V. Bazakutsa, A.M. Prokhorov, V.A. Sichugov, A.V. Tischenko, Pis'ma v Zh. Tekh. Fiz. (Sov. Phys. – Tech. Phys.) **10**, 1086 (1984)
[75] A.A. Samokhin, Kvantov. Elektron. (Sov. J. Quant. Electron.) **10**, 2022 (1983)
[76] V.I. Emel'yanov, V.N. Semigonov, E.M. Zemskov, Kvantov. Elektron. (Sov. J. Quant. Electron.) **10**, 2389 (1983)
[77] M.I. Tribel'skii, S.M. Gol'dberg, Pis'ma v Zh. Tekh. Fiz. (Sov. Phys. – Tech. Phys.) **8**, 1227 (1982)